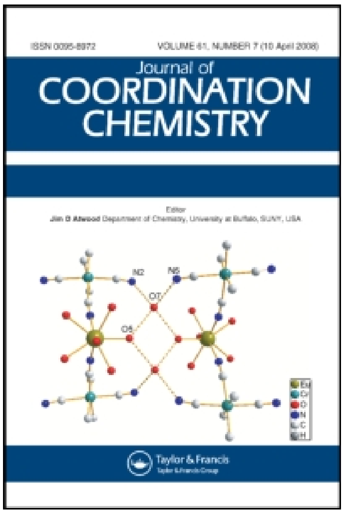

Journal of Coordination Chemistry
Publication details, including instructions for authors and subscription information:
http://www.informaworld.com/smpp/title~content=t713455674

SYNTHESIS, CHARACTERIZATION AND STRUCTURAL ANALYSES OF THREE LANTHANIDE CYANIDE-BRIDGED COMPLEXES

Donald F. Mullica[a]; J. Matt Farmer[a]; Brian P. Cunningham[a]; Jason A. Kautz[a]
[a] Department of Chemistry, Baylor University, Waco, TX, USA

To cite this Article Mullica, Donald F. , Farmer, J. Matt , Cunningham, Brian P. and Kautz, Jason A.(2000) 'SYNTHESIS, CHARACTERIZATION AND STRUCTURAL ANALYSES OF THREE LANTHANIDE CYANIDE-BRIDGED COMPLEXES', Journal of Coordination Chemistry, 49: 3, 239 — 250

To link to this Article: DOI: 10.1080/00958970008022575

URL: http://dx.doi.org/10.1080/00958970008022575

J. Coord. Chem., 2000, Vol. 49, pp. 239–250
Reprints available directly from the publisher
Photocopying permitted by license only

Published by license under
the Gordon and Breach Science
Publishers imprint.
Printed in Malaysia.

SYNTHESIS, CHARACTERIZATION AND STRUCTURAL ANALYSES OF THREE LANTHANIDE CYANIDE-BRIDGED COMPLEXES

DONALD F. MULLICA[†], J. MATT FARMER,
BRIAN P. CUNNINGHAM and JASON A. KAUTZ*

Department of Chemistry, Baylor University, Waco, TX 76798-7348, USA

(Received 31 December 1998; Revised 19 March 1999; In final form 15 July 1999)

Three lanthanide (Ln) complexes $(DMF)_4(H_2O)_3LnFe(CN)_6 \cdot H_2O$, where Ln = Er, Yb, and Lu, were structurally determined by means of three-dimensional single-crystal X-ray diffraction analysis. These systems crystallize in the centrosymmetric monoclinic space group $P2_1/c$ (No. 14) with $Z = 4$ and respective lattice constants of $a = 13.956(2), 13.952(1), 13.937(3)$; $b = 8.867(4), 8.864(1), 8.862(2)$; $c = 24.857(3), 24.812(2), 24.770(5)$ Å; and $\beta = 96.30(1)°, 96.33(1)°, 96.30(3)°$. Final least-squares full-matrix refinements based on 3499, 3367, and 2555 unique reflections yielded reliability (R) index factors of 0.071, 0.051, and 0.032, respectively. In each complex, the coordination about the central Ln ion is eight in a square-antiprism arrangement and the coordination about the Fe ions is six, oriented octahedrally. Cyanide bridging links the Ln ions to the FeC_6 groups. Molecules in the crystal lattice of each complex are held together by van der Waals forces and a network of hydrogen bonding. Characterization includes physical property determinations, conoscopical studies, thermal gravimetric analyses, and IR spectrometric identifications. Selected bond lengths and angles are tabularized and a synthesis of these compounds is presented.

Keywords: X-ray structure; lanthanide complexes; hexacyanides; cyanide bridging

INTRODUCTION

An excellent review of the chemistry of transition metal cyano complexes is in one of the series of monographs on organometallic chemistry.[1] However,

---

* Corresponding author. E-mail: Jason_Kautz@baylor.edu.

[†] Deceased 30 March 1999.

when considering lanthanide ferricyanides, it was Prandtl and Mohr[2] who first reported the synthesis of single crystals of $LnFe(CN)_6 \cdot nH_2O$. Milligan *et al.*[3] employing single-crystal X-ray diffractometry established the crystal structure of $LaFe(CN)_6 \cdot 5H_2O$. More recent research dealing with ferricyanide compounds has incorporated species such as copper diethylenetriamine,[4] nickel ethylenediamine,[5] and nickel 1,2-propanediamine and 1,1-dimethylethylenediamine.[6] Interesting studies of cyanide-bridged lanthanide-transition metals such as $(DMF)_{10}Yb_2[Ni(CN)_4]_3$ and $(DMF)_{10}Yb_2[Pt(CN)_4]_3$[7] and the single-crystal analyses of $(DMF)_4EuNi(CN)_4$ and $(DMF)_4EuPt(CN)_4$[8] have directed attention to the possibility of incorporating N,N-dimethylformamide into lanthanide ferrihexacyanide complexes. Most recent, a dinuclear cyano-bridged complex based on hexacyanoferrate and samarium nitrate was crystallographically studied,[9] $[Sm(DMF)_4(H_2O)_4Fe(CN)_6] \cdot H_2O$ where the central Sm atom is nine-coordinate with a distorted tricapped trigonal prism geometry. Interest in lanthanide-transition metal cyanides with varied amounts of hydration has been long standing in this laboratory dating back to the structural analysis of $LaKFe(CN)_6 \cdot 4H_2O$ in 1978.[10] We now report the results of the structural investigations of three $(DMF)_4(H_2O)_3LnFe(CN)_6 \cdot H_2O$ analogues which are eight-coordinate with a square-antiprism geometry about the central Ln atoms.

EXPERIMENTAL

Synthesis of $(DMF)_4(H_2O)_3LnFe(CN)_6 \cdot H_2O$; Ln = Er(I), Yb(II), and Lu(III)

The procedures for synthesizing (I), (II) and (III) were identical; 0.443 g (1.0 mmol), 0.449 g (1.0 mmol) and 0.451 g (1.0 mmol) of Er, Yb, and $Lu(NO_3)_3 \cdot 5H_2O$, respectively, were dissolved in N,N-dimethylformamide (10 mL, 0.1 mmol). An equimolar quantity of $K_3Fe(CN)_6$ (0.329 g, 1.0 mmol) was dissolved in distilled deionized water. Each of the Er, Yb, Lu/DMF solutions were layered onto separately prepared ferrihexacyanide solutions. After being covered and placed in the dark for approximately twenty-four hours, crystals of (I), (II), and (III) large enough for single-crystal X-ray analysis were obtained.

Physical Properties and Thermal Analyses

The experimental densities for (I), (II), and (III) were pycnometrically determined by employing the flotation method (bromobenzene, 2,3-dibromobutane) 1.603(4), 1.625(2), and 1.641(4) $\mathrm{Mg\,m^{-3}}$, respectively [calculated: (**I**), 1.611; (**II**), 1.628; (**III**), 1.637 $\mathrm{Mg\,m^{-3}}$]. Conoscopical examinations of each studied complex using crystal rotation between two polarizers on a Zeiss Photomicroscope II, served to determine the optical indicatrix which is related to the symmetry direction of a system of interest. The shapes of the indicatrix of (**I**), (**II**), and (**III**) were general ellipsoids demonstrating the biaxial (anisotropic, birefringent) character of each crystal system. The conoscopic surveys also confirmed the homogeneity of the selected crystals for X-ray diffraction analyses. A Perkin-Elmer TGS-1 thermobalance was used to ascertain the thermal decompositions of (**I**), (**II**), and (**III**). The instrument was run at 1.25°C $\mathrm{min^{-1}}$ while purging with N_2 (20 $\mathrm{cm^3\,min^{-1}}$). The analyses yielded a loss slightly greater than one water molecule per formula unit between 25°C and 100°C which can be assigned to the free water of hydration in each compound. Upon continuing to 110°C and then allowing the thermal balance to remain at this temperature for approximately 10 min, a loss of three more water molecules was observed. The thermal analyses of (**I**), (**II**), and (**III**) are in accordance with the following schematic:

$$2[A_4B_3C\cdot H_2O]\xrightarrow{25-100^\circ C}2[A_4B_3C]\xrightarrow{100-110^\circ C}2[A_4C]\xrightarrow{110-160^\circ C}2C\xrightarrow{160-200^\circ C}D$$

where $A=\mathrm{DMF}$, $B=(H_2O)$, $C=\mathrm{LnFe(CN)_6}$, and $D=\mathrm{Ln_2O_3/Fe_2O_3}$ (black). Note, that allowing samples of each studied complex to remain (without heat) overnight in a weighing pan of the thermal balance, a weight loss equivalent to more than four water molecules was recorded. For this reason, special care would be needed for data collection.

IR Spectra of (I), (II), and (III)

Infrared spectral data were recorded on a Mattson-Cygnus 100 FTIR analyzer over the frequency range of 4000–400 $\mathrm{cm^{-1}}$ using the KBr pellet technique (pressed to 20 klb in^2). The spectra for each compound were similar displaying the following notable identification peaks: very broad bands at 3350 $\mathrm{cm^{-1}}$ (ν-OH, hydrogen bonding), sharp peaks at 2943 $\mathrm{cm^{-1}}$ (C–H stretch, ν-CH_3) three very sharp peaks at 2156, 2144, and 2124 (ν-C≡N), sharp peaks at 1654 $\mathrm{cm^{-1}}$ (δ-HOH), peaks at 1437 (C–H stretches, δ_{as}-CH_3) and 1383 $\mathrm{cm^{-1}}$ (C–H stretches, δ_s-CH_3), peaks at 1382 $\mathrm{cm^{-1}}$ (aldehydic C–H bend), peaks at 1058 $\mathrm{cm^{-1}}$ (C–N stretches), and peaks at 450 $\mathrm{cm^{-1}}$ (ν-Fe–C).

Single-Crystal Analyses of (I), (II), and (III)

Clear, yellow parallelepiped single crystals of each system selected on the basis of optical purity were encapsulated in glass capillaries to prevent decomposition and/or dehydration. The capillaries were then mounted on goniometer heads which in turn, were placed on an Enraf-Nonius (CAD-4F) diffractometer equipped with a dense graphite monochromator (take-off angle 2.8°). Using MoK$_{\bar{\alpha}}$ radiation ($\lambda_{\text{mean}} = 0.71073$ Å), the orientation matrices and initial cell dimensions were obtained through the application of subroutines SEARCH and INDEX which are part of the CAD4 operating system. Final lattice constants were determined from least-squares refinements of high angular settings, $30.0° \leq 2\theta \leq 50.0°$ (see Table I). Data were collected over the ranges of $1.5° < \theta < 25.0°$ for (I) and (II) and $1.5° < \theta < 20.0°$ for (III) utilizing the ω–2θ scan technique at scan rates between 1.18° and 4.12° min^{-1}. No significant variations (< 1.0%) were observed in the intensities of the monitored standards (three at 2 h intervals). Thus, electronic

TABLE I Crystal data and summaries of compound **I**, **II**, and **III**

	I	II	III
Crystal system	Monoclinic	Monoclinic	Monoclinic
Space group	$P2_1/c$	$P2_1/c$	$P2_1/c$
Crystal size (mm)	0.24 × 0.24 × 0.19	0.19 × 0.43 × 0.11	0.67 × 0.49 × 0.49
M_r	741.7	747.4	749.4
a (Å)	13.956(2)	13.952(1)	13.937(3)
b (Å)	8.867(4)	8.864(1)	8.862(2)
c (Å)	24.857(3)	24.812(2)	24.770(5)
β (°)	96.30(1)	96.33(1)	96.30(1)
V (Å^3)	3057.4(15)	3049.8(5)	3040.9(11)
Z	4	4	4
D_m (Mg m^{-3})	1.603(4)	1.625(2)	1.641(4)
D_c (Mg m^{-3})	1.611	1.628	1.637
$F(000)$ (e$^-$)	1488	1496	1500
μ(MoK$_{\bar{\alpha}}$) (mm^{-1})	3.289	3.566	3.762
$\Delta 2\theta$ (°)	3.0–50.0	3.0–50.0	3.0–40.0
Scan range (ω, °)	$1.15 + 0.34 \tan\theta$	$1.15 + 0.34 \tan\theta$	$1.15 + 0.34 \tan\theta$
T(K)	291	291	291
Observed data	3499	3367	2555
R_{int}	0.025	0.040	0.013
Transmission range			
Min.	0.382	0.445	0.216
Max.	0.429	0.986	0.256
Refined parameters	344	344	344
Data to para. ratio	10.2 : 1	9.8 : 1	7.4 : 1
R, R_w	0.071(0.113)	0.051(0.052)	0.032(0.051)
g (10^{-4} e^{-2})	6.1(12)	1.2(2)	5.8(6)
GOF ($\sum_2$)	1.10	1.05	1.07

reliability, X-ray measurements, and crystal stabilities were assured for the studied systems. Totals of 5595, 5574, and 2921 intensity data were measured of which 5353, 5337, and 2830 were independent and 3499, 3367, and 2555 data with $F > 4.0\sigma(F)$ were included in the structure refinements of (**I**), (**II**), and (**III**), respectively ($R_{\text{int}} = 0.025$, 0.040, and 0.013). All resultant intensity data were corrected for Lorentz and polarization effects after which semi-empirical corrections were applied,[11] see Table I for transmission ranges. Examination of the treated data (**I**, **II**, and **III**) revealed systematic absences that are consistent with the monoclinic space group $P2_1/c$ ($h0l$: $l = 2n+1$ and $0k0 = 2n+1$). $N(Z)$ analyses (cumulative probability distributions relative to centrosymmetry test) provide evidence that the investigated systems are centrosymmetric in nature. The presence of any additional symmetry in (**I**), (**II**), and (**III**) was ruled out by employing the program MISSYM.[12]

The phase problems were resolved by using the heavy-atom (Patterson) method[11] which revealed the positions of the lanthanide and Fe ions in each data set. Difference Fourier mapping disclosed all the other non-hydrogen atomic positions. The hydrogen atoms in the three systems were generated for those associated with carbon atoms and coordinated water oxygen atoms, but not for those associated with the free water of hydration. The calculated H-atoms were held at C–H = 0.96 Å and O–H = 0.85 Å and constrained to ride on their respective bonding atoms with fixed isotropic thermal parameters, $U_{\text{iso}} = 80 \times 10^{-3}$ Å^2. All non-hydrogen atoms were refined anisotropically using the full-matrix least-squares procedure.[11] After several cycles of refinement of (**I**), (**II**), and (**III**) which included secondary extinction corrections (g), final reliability (R, R_w) index factors were obtained, $R = \sum \Delta F / \sum F_o$ and $R_w = [\sum w(\Delta F)^2 / \sum w(F_o)^2]^{1/2}$ where $\Delta F = ||F_o| - |F_c||$ and $w = \sigma^{-2}(F_o)$, see Table I. The 'goodness-of-fit' parameter is defined as $\sum_2 = \text{GOF} = [\sum w(\Delta F)^2 / N_G]^{1/2}$ where ΔF and w have been defined above and $N_G = (N_o - N_v)$, N_o is the number of independent observations and N_v is the number of varied parameters in each refinement. Final residual density maps revealed some density in the vicinity of the lanthanide atoms which is quite reasonable for heavy metal atom compounds. Elsewhere, the maps were featureless revealing only random fluctuating backgrounds. The minimized quantity in each refinement was $\sum w(|F_o| - |F_c|)^2$ and the weighting function $w = [\sigma^2(F) + BF^2]^{-1}$ where $B = 7.7 \times 10^{-3}$ for (**I**), 3.0×10^{-4} for (**II**), and 2.1×10^{-3} for (**III**). Atomic scattering factors for all non-hydrogen atoms were taken from the work of Ibers and Hamilton.[13] Final atomic positions and equivalent isotropic thermal parameters with estimated standard deviations (esds) are listed in

TABLE II Atomic coordinates ($\times 10^4$) and equivalent isotropic displacement coefficients ($\text{Å}^2 \times 10^3$) for I with esds in parentheses

Atom	*x*	*y*	*z*	U_{eq}[a]
Er	2569(1)	935(1)	1497(1)	24(1)
O(11)	1545(8)	1735(17)	746(6)	44(5)
C(11)	705(11)	2008(35)	668(10)	83(13)
N(11)	203(13)	2299(27)	212(9)	66(8)
C(12)	−825(22)	2473(61)	122(16)	153(25)
C(13)	714(25)	2152(72)	−260(15)	195(34)
O(21)	1129(10)	−371(15)	1549(6)	42(5)
C(21)	920(14)	−1656(19)	1650(9)	45(7)
N(21)	103(12)	−2249(20)	1698(8)	46(6)
C(22)	−779(20)	−1358(37)	1671(14)	89(14)
C(23)	10(22)	−3838(28)	1828(14)	84(12)
O(31)	4094(9)	−116(15)	1715(6)	43(5)
C(31)	4871(10)	−580(23)	1624(8)	39(7)
N(31)	5168(11)	−2008(20)	1731(7)	41(6)
C(32)	4633(25)	−3064(37)	2014(13)	92(14)
C(33)	6085(18)	−2565(32)	1599(12)	73(11)
O(41)	2633(11)	−1230(16)	958(6)	49(5)
C(41)	3191(16)	−1607(28)	647(8)	59(9)
N(41)	3408(13)	−2994(23)	496(8)	54(7)
C(42)	4123(23)	−3323(52)	159(16)	164(23)
C(43)	2924(30)	−4172(39)	741(17)	126(21)
O(51)	3506(9)	1901(16)	854(5)	42(5)
O(61)	3523(8)	2895(15)	1923(6)	40(4)
O(71)	1582(9)	2750(14)	1859(6)	42(5)
Fe	2563(2)	−2263(3)	3354(1)	23(1)
C(81)	2566(11)	−854(21)	2759(6)	28(5)
N(81)	2582(10)	−82(18)	2392(6)	35(5)
C(82)	2426(13)	−687(22)	3858(7)	40(7)
N(82)	2344(16)	234(21)	4172(8)	64(8)
C(83)	2591(12)	−3735(19)	3928(7)	32(6)
N(83)	2658(16)	−4630(22)	4266(7)	63(8)
C(84)	2640(13)	−3893(18)	2849(6)	32(6)
N(84)	2676(12)	−4812(19)	2524(7)	44(6)
C(85)	1206(9)	−2396(20)	3239(7)	26(5)
N(85)	376(10)	−2387(22)	3153(8)	53(7)
C(86)	3955(10)	−2061(22)	3500(7)	33(6)
N(86)	4775(9)	−1870(21)	3583(9)	57(7)
O(91)	6730(11)	7656(17)	213(5)	51(5)

[a] Equivalent isotropic *U* defined as one third of the trace of the orthogonalized U_{ij} tensor.

Tables II–IV. Structure factor tables are available from the authors (J.A.K.).

RESULTS AND DISCUSSION

Table V lists bond lengths and pertinent bond angles for (**I**), (**II**), and (**III**). Figure 1 is a representative molecular view of the three cyanide-bridged

TABLE III Atomic coordinates ($\times 10^4$) and equivalent isotropic displacement coefficients ($\text{Å}^2 \times 10^3$) for II with esds in parentheses

Atom	*x*	*y*	*z*	U_{eq}[a]
Yb	2567(1)	932(1)	1499(1)	18(1)
O(11)	1567(7)	1757(12)	752(4)	38(4)
C(11)	715(9)	1966(22)	660(8)	60(7)
N(11)	203(9)	2238(19)	204(5)	56(6)
C(12)	−817(14)	2526(39)	144(11)	143(16)
C(13)	651(17)	2236(47)	−262(9)	180(21)
O(21)	1108(7)	−343(12)	1541(4)	39(4)
C(21)	942(12)	−1637(15)	1653(7)	49(7)
N(21)	112(8)	−2255(15)	1699(5)	37(4)
C(22)	−754(14)	−1344(19)	1677(10)	75(9)
C(23)	26(15)	−3842(19)	1838(9)	77(9)
O(31)	4088(6)	−99(11)	1716(4)	35(3)
C(31)	4851(9)	−627(21)	1617(6)	53(7)
N(31)	5165(8)	−2014(13)	1732(5)	31(4)
C(32)	4638(16)	−3018(29)	2025(9)	94(11)
C(33)	6067(13)	−2582(26)	1580(8)	85(10)
O(41)	2627(8)	−1198(11)	967(4)	43(4)
C(41)	3189(11)	−1585(21)	657(7)	57(7)
N(41)	3398(11)	−2981(19)	524(7)	64(6)
C(42)	4080(16)	−3353(30)	156(9)	118(13)
C(43)	2898(20)	−4236(25)	745(12)	143(16)
O(51)	3497(6)	1881(12)	855(4)	34(3)
O(61)	3498(6)	2887(11)	1921(4)	37(4)
O(71)	1587(6)	2707(11)	1863(4)	35(3)
Fe	2570(1)	−2256(2)	3354(1)	17(1)
C(81)	2579(8)	−834(16)	2754(4)	22(4)
N(81)	2592(7)	−47(13)	2390(4)	29(4)
C(82)	2449(9)	−617(14)	3862(5)	26(5)
N(82)	2356(9)	311(14)	4172(5)	41(5)
C(83)	2650(9)	−3910(16)	2840(5)	27(4)
N(83)	2679(9)	−4854(15)	2523(5)	49(5)
C(84)	2615(10)	−3738(15)	3930(5)	29(5)
N(84)	2682(11)	−4574(16)	4286(6)	59(6)
C(85)	1178(8)	−2369(14)	3216(5)	23(4)
N(85)	353(8)	−2415(15)	3143(5)	44(5)
C(86)	3956(7)	−2059(12)	3491(5)	21(5)
N(86)	4764(9)	−1906(14)	3582(5)	40(4)
O(91)	6740(8)	7697(13)	204(4)	50(4)

[a] Equivalent isotropic *U* defined as one third of the trace of the orthogonalized U_{ij} tensor.

lanthanide complexes showing the crystallographic numbering scheme. The crystal structure of these systems is comprised of four DMF groups, three water molecules and a discrete hexacyanoferrate (III) group, all bonded to a central Ln ion. The eight-coordinate (CN = 8) geometry about Er, Yb and Lu ions is a square antiprism (D_{4d}) and the six-coordination (CN = 6) about the Fe ions is octahedral (O_h). The mean Er–O, Yb–O, and Lu–O distances of 2.35(1), 2.33(1), and 2.32(1) Å are in direct agreement with the summation of the radii of Er(CN = 8, 1.004 Å), Yb(CN = 8, 0.985 Å),

TABLE IV Atomic coordinates ($\times 10^4$) and equivalent isotropic displacement coefficients ($Å^2 \times 10^3$) for III with esds in parentheses

Atom	*x*	*y*	*z*	U_{eq}[a]
Lu	2565(1)	926(1)	1499(1)	38(1)
O(11)	1563(4)	1729(6)	750(2)	59(2)
C(11)	724(7)	1986(12)	666(4)	83(5)
N(11)	209(5)	2243(10)	205(3)	72(3)
C(12)	−810(8)	2540(20)	137(6)	142(8)
C(13)	693(10)	2179(21)	−283(6)	151(9)
O(21)	1114(4)	−333(6)	1547(2)	54(2)
C(21)	950(7)	−1633(10)	1646(4)	68(4)
N(21)	108(5)	−2258(7)	1699(3)	54(3)
C(22)	−751(8)	−1395(13)	1669(6)	106(6)
C(23)	−24(8)	−3855(11)	1812(5)	93(5)
O(31)	4078(4)	−95(6)	1717(2)	59(2)
C(31)	4839(7)	−633(12)	1611(4)	76(5)
N(31)	5153(4)	−2013(7)	1734(3)	47(2)
C(32)	4656(9)	−3060(14)	2030(5)	112(6)
C(33)	6069(7)	−2562(14)	1583(5)	95(5)
O(41)	2620(4)	−1224(6)	982(3)	61(2)
C(41)	3185(6)	−1578(11)	660(4)	70(4)
N(41)	3384(6)	−2975(10)	518(4)	81(4)
C(42)	4056(10)	−3377(20)	147(6)	150(8)
C(43)	2893(12)	−4225(14)	731(6)	134(8)
O(51)	3501(4)	1876(6)	858(2)	57(2)
O(61)	3503(3)	2870(5)	1914(2)	53(2)
O(71)	1599(3)	2700(6)	1863(2)	56(2)
Fe	2570(1)	−2264(1)	3351(1)	38(1)
C(81)	2581(5)	−857(8)	2755(3)	43(3)
N(81)	2603(4)	−68(8)	2393(3)	53(3)
C(82)	2437(6)	−632(10)	3862(3)	45(3)
N(82)	2354(5)	292(9)	4174(3)	70(3)
C(83)	2606(6)	−3735(10)	3936(4)	50(3)
N(83)	2669(6)	−4602(10)	4287(4)	78(3)
C(84)	2654(6)	−3907(9)	2835(4)	50(3)
N(84)	2680(5)	−4864(9)	2524(3)	68(3)
C(85)	1180(6)	−2376(8)	3227(3)	44(3)
N(85)	356(5)	−2410(8)	3147(3)	62(3)
C(86)	3952(6)	−2055(8)	3489(3)	46(3)
N(86)	4772(5)	−1896(9)	3581(3)	70(3)
O(91)	6727(4)	7670(7)	198(2)	67(2)

[a]Equivalent isotropic *U* defined as one third of the trace of the orthogonalized U_{ij} tensor.

Lu(CN = 8, 0.977 Å) and that of oxygen 1.35(1) Å, all obtained from the work of Shannon.[14] The mean C≡N bond length of 1.148(5) Å (range, 1.140–1.156 Å) is also in direct accord with the sum of the triple bond radii of C and N atoms (0.603 and 0.55 Å, respectively) found in the work of Pauling.[15] The same holds true for the overall mean Fe–C distance in (**I**), (**II**), and (**III**), 1.93(2) Å (see Table V) when compared to r(Fe) + r(C) = 1.94 Å also obtained from the *Nature of the Chemical Bond.*[15] Experimental comparisons of Fe–C bond lengths can be found in the structural

TABLE V Selected internuclear distances (Å) and angles (°) with esds in parentheses for **I**, **II**, and **III**

	I	II	III
Ln–O(11)	2.333(13)	2.311(8)	2.308(5)
Ln–O(21)	2.335(14)	2.330(9)	2.325(6)
Ln–O(31)	2.333(12)	2.317(7)	2.303(6)
Ln–O(41)	2.347(15)	2.323(9)	2.302(6)
Ln–O(51)	2.336(14)	2.326(8)	2.320(6)
Ln–O(61)	2.368(13)	2.345(8)	2.333(5)
Ln–O(71)	2.361(13)	2.325(8)	2.316(5)
Ln–N(81)	2.398(14)	2.374(10)	2.379(7)
Fe–C(81)	1.936(16)	1.948(11)	1.934(8)
Fe–C(82)	1.901(18)	1.940(12)	1.944(9)
Fe–C(83)	1.932(18)	1.954(12)	1.946(9)
Fe–C(84)	1.925(13)	1.934(11)	1.950(8)
Fe–C(85)	1.888(13)	1.938(10)	1.930(8)
Fe–C(86)	1.945(13)	1.932(9)	1.927(8)
$C\equiv N$(mean)	1.150(5)	1.146(4)	1.147(6)
O–C(sp^2, mean)	1.202(6)	1.209(5)	1.208(13)
N–C(sp^2, mean)	1.311(30)	1.305(11)	1.316(10)
N–C(sp^3, mean)	1.435(18)	1.433(26)	1.435(16)
O(91)···O(51)	2.640	2.637	2.631
O(91)···N(82)	2.853	2.845	2.839
O(91)···N(83)	2.824	2.808	2.818
Ln–N(81)$\equiv$C(81)	165.2(14)	164.4(9)	163.7(7)
Fe–$C\equiv N$(mean)	176.6(8)	177.4(6)	177.9(4)
Ln–O(11)–C(11)	134.2(16)	134.2(10)	134.2(6)
Ln–O(21)–C(21)	135.0(13)	131.3(9)	130.9(6)
Ln–O(31)–C(31)	155.5(13)	155.1(9)	154.1(6)
Ln–O(41)–C(41)	131.4(15)	131.2(9)	129.7(6)

investigations of $TrFe(CN)_5NO \cdot 3H_2O$ where Tr = Zn, Mn, and Cd, Fe–C (mean) = 1.933(8), 1.935(5), and 1.942(6) Å, respectively.[16,17] All bond distances in (**I**), (**II**), and (**III**) are in agreement with published values.[18,19] The overall mean O–C(sp^2), N–C(sp^2), and N–C(sp^3) bond lengths in the DMF/cyano complexes are 1.206(9), 1.31(2), and 1.44(2) Å. The interaction of Fe 3*d* orbitals and the $C\equiv N^-$ orbitals leads to strong directional bonding; the Fe–$C\equiv N^-$ angles in (**I**), (**II**), and (**III**) are approximately 177°, see Table V. However, little or no directional influences are observed concerning electrostatic bonding of the Ln ions to the $C\equiv N^-$ groups; the mean overall Ln–$N\equiv C$ angle in the three data sets is 164.4°.

Hydrogen bonding and van der Waals cohesive forces are of paramount importance in the intermolecular network of the crystal lattices of these complexes. The molecular units within the crystal lattice of each system are separated by normal van der Waals contact distances. According to the work of Hamilton and Ibers,[20] hydrogen bonding of the O–H···N and

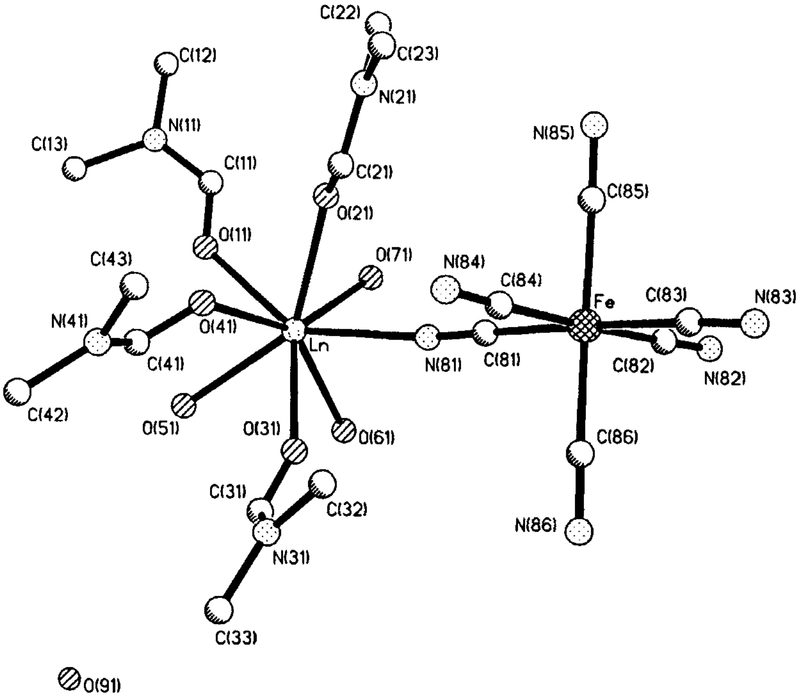

FIGURE 1 A representive molecular view of **I**, **II**, and **III** showing the crystallographic numbering scheme and displaying the eight-coordination and six-coordination about the Ln and Fe ions, respectively. Note, the square antiprism (SAP) and octahedral geometries and the cyanide bridging connecting the Ln and Fe ions. Hydrogen atoms have been eliminated for clarity.

O–H···O types may be present when O···N and O···O contact distances are within 3.2 Å, see Table V. Such is the case here in the crystal lattices of (**I**), (**II**), and (**III**) where the free water of hydration, O(91), is involved in the hydrogen bonding network, see Figure 2. The IR spectrum of each compound yields evidence of hydrogen bonding (see Experimental section, *IR spectra*).

Interest in these lanthanide cyanide-bridged complexes will continue due to their possible ability to function as ideal models for evaluating molecule–membrane interactions and molecular transport in permselective membranes. Both selectivity and permeation rates of the species of interest can be strongly influenced by the molecular structure of exchange host. The development of new materials with such possibilities is always of interest to this research laboratory.

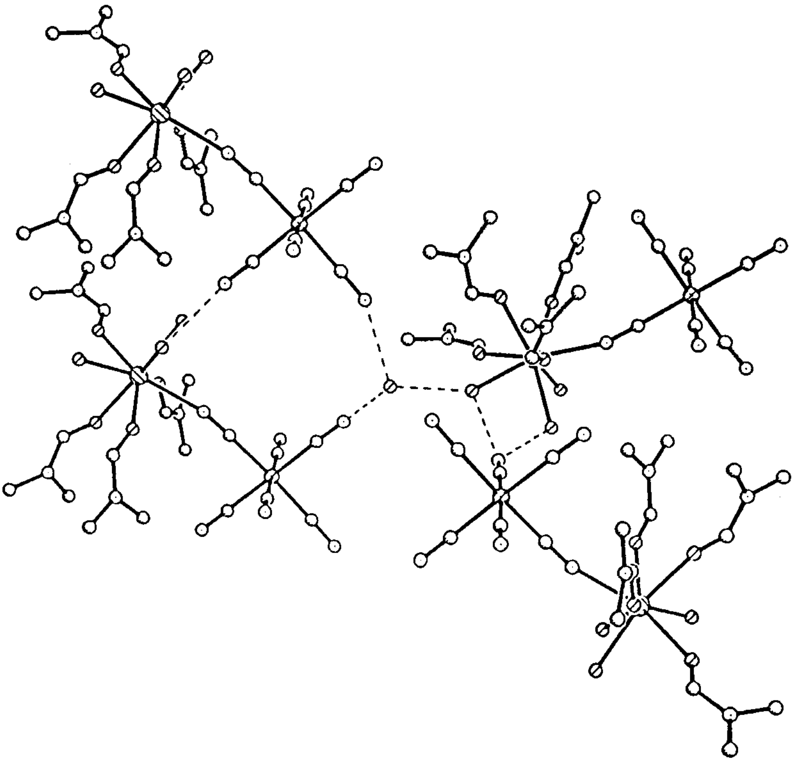

FIGURE 2 A representative view of **I**, **II**, and **III** displaying the network of hydrogen bonding involving the free water of hydration, O(91), and that involving N···O hydrogen bonding interaction.

Acknowledgments

The authors gratefully acknowledge the financial support of The Robert A Welch Foundation (Grant No. AA-0668) and Baylor University (URC, 001-S98).

Supplementary Materials

Anisotropic thermal parameters, H-atom coordinates, complete bond distance and angles, and structure factor data are available from the authors (J.A.K.).

References

[1] A.G. Sharpe, *The Chemistry of Cyano Complexes of the Transition Metals* (Academic Press, NY 1976).

[2] W. Prandtl and S. Mohr, *Z. Anorg. Alleg. Chem.*, **236**, 243 (1938).
[3] W.E. Bailey, R.J. Williams and W.O. Milligan, *Acta Crystallogr.*, **B29**, 1365 (1973).
[4] G.O. Morpurgo, V. Mosini, P. Porta, G. Dessy and V. Fares, *J. Chem. Soc., Dalton Trans.*, 1272 (1980).
[5] M. Ohba, N. Maruone, H. Okawa, T. Enoki and J.-M. Latour, *J. Am. Chem. Soc.*, **116**, 11 566 (1994).
[6] M. Ohba, H. Okawa, N. Fukita and Y. Hashimoto, *J. Am. Chem. Soc.*, **119**, 1011 (1997).
[7] D.W. Knoeppel and S.G. Shore, *Inorg. Chem.*, **35**, 1747 (1996).
[8] D.W. Knoeppel and S.G. Shore, *Inorg. Chem.*, **35**, 5328 (1996).
[9] H.-Z. Kou, G.-M. Yang, D.-Z. Liao, P. Cheng, Z.-H. Jiang, S.-P. Yan, X.-Y. Huang and G.-L. Wang, *J. Chem. Crystallogr.*, **28**, 303 (1998).
[10] G.W. Beall, D.F. Mullica and W.O. Milligan, *Acta Crystallogr.*, **B34**, 1446 (1978).
[11] SHELXTL-PC, Siemens Analytical X-ray Instruments, Madison, WI, USA (1989).
[12] E.J. Gabe, Y. LePage, J.-P. Charland and F.L. Lee, *J. Appl. Crystallogr.*, **22**, 384 (1989).
[13] J.A. Ibers and W.C. Hamilton, *International Tables for X-ray Crystallography*, Vol. IV (Kynoch Press, Birmingham, U.K. 1974).
[14] R.D. Shannon, *Acta Crystallogr.*, **A32**, 751 (1976).
[15] L. Pauling, *The Nature of the Chemical Bond*, 3rd edn. (Cornell Univ. Press, New York 1960).
[16] D.F. Mullica, E.L. Sapenfield, D.B. Tippin and D.H. Leschnitzer, *Inorg. Chim. Acta*, **164**, 99 (1989).
[17] D.F. Mullica, D.B. Tippin and E.L. Sapenfield, *Inorg. Chim. Acta*, **174**, 129 (1990).
[18] A.G. Orpen, L. Brammer, F.H. Allen, O. Kennard, D.G. Watson and R. Taylor, *J. Chem. Soc., Dalton Trans.*, **S1** (1989).
[19] BIDICS, Institute for Material Research, Hamilton Canada (1969–1981).
[20] W.C. Hamilton and J.A. Ibers, *Hydrogen Bonding in Solids* (W.A. Benjamin, Inc., N.Y.C., NY, 1968).